Article

Chiral Ethylhexyl Substituents for Optically Active Aggregates of π-Conjugated Polymers

Christophe R. G. Grenier, Subi J. George, Thomas J. Joncheray, E. W. Meijer, and John R. Reynolds

J. Am. Chem. Soc., **2007**, 129 (35), 10694-10699• DOI: 10.1021/ja068461t • Publication Date (Web): 09 August 2007

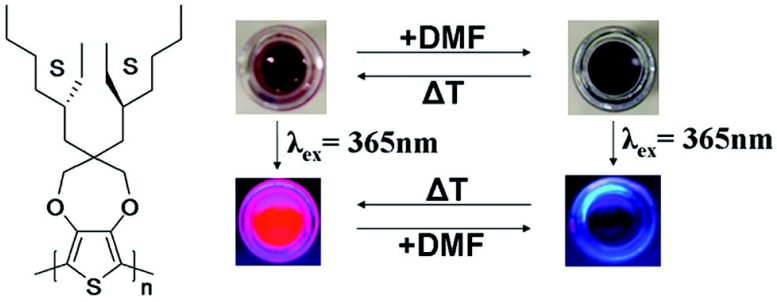

More About This Article

Additional resources and features associated with this article are available within the HTML version:

- Supporting Information
- Links to the 5 articles that cite this article, as of the time of this article download
- Access to high resolution figures
- Links to articles and content related to this article
- Copyright permission to reproduce figures and/or text from this article

View the Full Text HTML

J|A|C|S
ARTICLES
Published on Web 08/09/2007

Chiral Ethylhexyl Substituents for Optically Active Aggregates of π-Conjugated Polymers

Christophe R. G. Grenier,[†] Subi J. George,[‡] Thomas J. Joncheray,[†] E. W. Meijer,[‡] and John R. Reynolds*,[†]

Contribution from The George and Josephine Butler Polymer Laboratory, Department of Chemistry, Center for Macromolecular Science and Engineering, Gainesville, Florida 32611-7200, and Laboratory of Macromolecular and Organic Chemistry, Technische Universiteit Eindhoven, P.O. Box 513, 5600 MB Eindhoven, The Netherlands

Received November 25, 2006; Revised Manuscript Received June 24, 2007; E-mail: reynolds@chem.ufl.edu

Abstract: We report an efficient synthesis of chiral (2*S*)-ethylhexanol for functionalizing and solubilizing conjugated polymers. The α-substituted chiral ethylhexyl side chains were obtained through a powerful and flexible asymmetric synthesis using pseudoephedrine as a chiral auxiliary. The dependence of the properties of conjugated polymers on molecular structure is investigated by circular dichroism, fluorescence, and absorption spectroscopy on two new chiral conjugated polymers, poly(3,3-bis((*S*)-2-ethylhexyl)-3,4-dihydro-2H-thieno[3,4-b][1,4]dioxepine) (PProDOT((2*S*)-ethylhexyl)$_2$) and poly(3,3-bis((*S*)-2-methylbutyl)-3,4-dihydro-2H-thieno[3,4-b][1,4]dioxepine) (PProDOT((2*S*)-methylbutyl)$_2$). The properties of PProDOT((2*S*)-ethylhexyl)$_2$) differ significantly from those of its methylbutyl analog as investigated by chiral aggregation providing insight into the role of interchain interactions in these subsecond switching electrochromic polymers.

Introduction

Substitution with branched alkyl chains is a highly effective method for inducing solubility in otherwise insoluble conjugated polymers (CPs) as their bulkiness efficiently reduces interchain interactions. CPs substituted with 2-ethylhexyl side chains have been widely used, such as poly(2-methoxy,5-(2-ethylhexyloxy),1,4-phenylenevinylene) (MEH−PPV) which is one of the most studied and efficient polymers in light-emitting and photovoltaic applications.[1] Recently, our research group reported the synthesis of spray processable, regiosymmetric ethylhexyl-substituted poly(3,4-propylenedioxythiophene)s, including PProDOT-(2-ethylhexyl)$_2$ and PProDOT-(CH_2O-2-ethylhexyl)$_2$.[2,3] These polymers were used in the fabrication of high-contrast, subsecond switching and high coloration efficiency electrochromic (EC) devices. Similar polymers substituted with linear alkyl chains yielded poorer EC properties.[4] It was observed that the 2-ethylhexyl-substituted polymers undergo a very sharp transition in luminance and absorption spectrum as a function of potential.

The use of circular dichroism (CD) spectroscopy provides a powerful tool for examining aggregation and ordering behavior in CPs.[5] Here, we report on the first chiral ethylhexyl-functionalized PProDOTs with EC switching comparable to its racemic analogues and a sharp transition as a function of potential.[3] The impact of the chemistry we report in synthesizing the side-chain precursor is of broad interest as, to date, only one CP, a polyfluorene with chiral 2-ethylhexyl side chains, has been reported.[6] In that case, the side chain was obtained by enzymatic catalysis giving low yields (10%) and providing little flexibility (only one enantiomer is accessible) in preparing analogues.

In this work, two soluble enantiomerically pure disubstituted poly(3,4-propylenedioxythiophenes) (PProDOTs), PProDOT-((2*S*)methylbutyl))$_2$ (**P1**) and PProDOT-((2*S*)-ethylhexyl)$_2$ (**P2**) were synthesized by Grignard metathesis polymerization.[7] Chiral (2*S*)-ethylhexanol (**4**) was obtained by enantioselective alkylation of an acylated pseudoephedrine, modifying a procedure outlined by Myers and co-workers .[8] This flexible method, using inexpensive materials, gives high yields and allows the efficient synthesis of a variety of chiral primary alcohols with variable substituents on the α-position, along with other derivatives including chiral acids, acyl chlorides, and aldehydes. Both enantiomeric products can be obtained by using either enantiomerically pure *d*- or *l*-pseudoephedrine.

[†] University of Florida.
[‡] Technische Universiteit Eindhoven.

(1) (a) Hoppe, H.; Glatzel, T.; Niggemann, M.; Schwinger, W.; Schaeffler, F.; Hinsch, A.; Lux-Steiner, M. C.; Sariciftci, N. S. *Thin Solid Films* **2006**, *511*−*512*, 587−592. (b) Friend, R. H.; Gymer, R. W.; Holmes, A. B.; Burroughes, J. H.; Marks, R. N.; Taliani, C.; Bradley, D. D. C.; Dos Santos, D. A.; Bredas, J. L.; Logdlund, M.; Salaneck, W. R. *Nature* **1999**, *397*, 121−128. (c) Sirringhaus, H.; Tessler, N.; Friend, R. H. *Science* **1998**, *280*, 1741−1744. (d) Kraft, A.; Grimsdale, A. C.; Holmes, A. B. *Angew. Chem., Int. Ed.* **1998**, *37*, 402−428.
(2) Welsh, D. M.; Kloeppner, L. J.; Madrigal, L.; Pinto, M. R.; Thompson, B. C.; Schanze, K. S.; Abboud, K. A.; Powell, D.; Reynolds, J. R. *Macromolecules* **2002**, *35*, 6517−6525.
(3) Reeves, B. D.; Grenier, C. R. G.; Argun, A. A.; Cirpan, A.; McCarley, T. D.; Reynolds, J. R. *Macromolecules* **2004**, *37*, 7559−7569.
(4) Cirpan, A.; Argun, A. A.; Grenier, C. R. G.; Reeves, B. D.; Reynolds, J. R. *J. Mater. Chem.* **2003**, *13*, 2422−2428.
(5) Zahn, S.; Swager, T. M. *Angew. Chem., Int. Ed.* **2002**, *41*, 4225−4230.
(6) Oda, M.; Nothofer, H. G.; Scherf, U.; Sunjic, V.; Richter, D.; Regenstein, W.; Neher, D. *Macromolecules* **2002**, *35*, 6792−6798.
(7) Loewe, R. S.; Khersonsky, S. M.; McCullough, R. D. *Adv. Mater.* **1999**, *11*, 250.
(8) (a) Myers, A. G.; Yang, B. H.; Chen, H.; Gleason, J. L. *J. Am. Chem. Soc.* **1994**, *116*, 9361−9362. (b) Myers, A. G.; Yang, B. H.; Chen, H.; McKinstry, L.; Kopecky, D. J.; Gleason, J. L. *J. Am. Chem. Soc.* **1997**, *119*, 6496−6511.

10.1021/ja068461t CCC: $37.00

Scheme 1. Synthesis of (2*S*)-Ethylhexanol from *l*-Pseudoephedrine

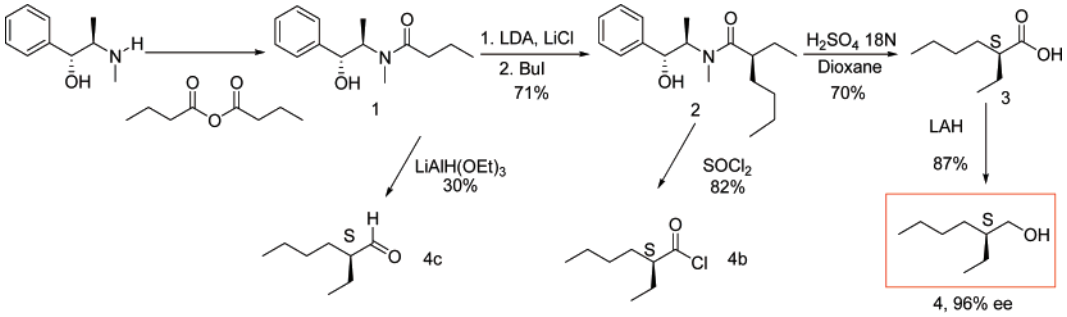

Scheme 2. Synthesis of Chiral Polymers **P1** and **P2** from Enantiomerically Pure (2*S*)-Methylbutanol and (2*S*)-Ethylhexanol

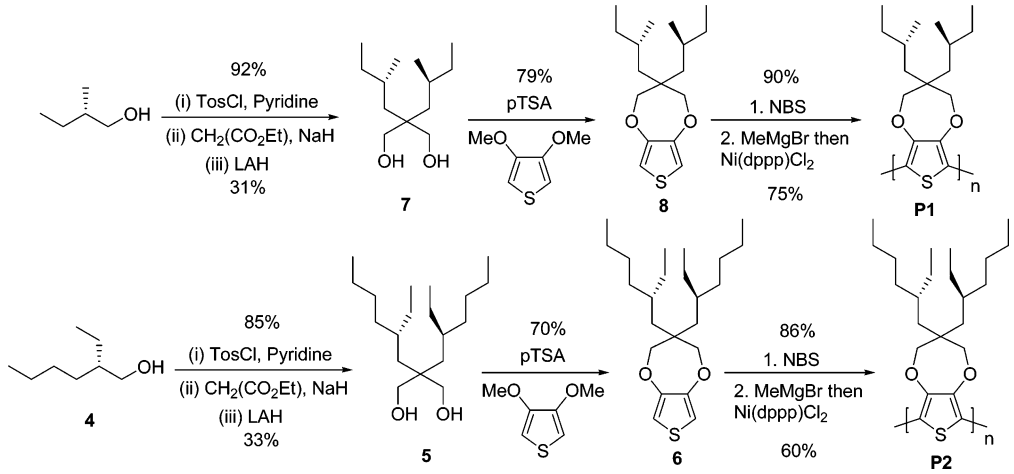

Results and Discussion

Synthesis and Characterization. Chiral (2*S*)-ethylhexanol was prepared as described in Scheme 1 starting by the acylation of (1*R*,2*R*)-pseudoephedrine using butyric anhydride. Diastereoselective alkylation of the enolate generates **2**, which can be hydrolyzed under acidic conditions to give (2*S*)-chiral ethylhexanoic acid. Reduction with lithium aluminum hydride yields (2*S*)-ethylhexanol. The enantiomeric excess was determined by chiral GC of the Mosher ester, being 96% (see the Supporting Information). (2*S*)-Ethylhexanal and (2*S*)-ethylhexanoyl chloride, useful intermediates in Wittig or Friedel−Craft reactions, were also synthesized, demonstrating the versatility of the synthesis.

Both monomers for **P1** and **P2** were obtained by a modified procedure used for the synthesis of the racemic ProDOTs and described in Scheme 2.[3] For **P1**, commercial (2*S*)-methylbutanol was used. After tosylation of the chiral alcohols, malonic ester synthesis was carried out to yield, after $LiAlH_4$ reduction, intermediates **5** and **7**. Transetherification of **7** and **5** with 3,4-dimethoxythiophene afforded oxidatively polymerizable ProDOT((2*S*)-methylbutyl)$_2$ (**8**) and ProDOT((2*S*)-ethylhexyl)$_2$ (**6**). Following bromination with NBS, the polymers **P1** and **P2** were obtained by nickel-catalyzed Grignard metathesis polymerization.[7]

After Soxhlet extraction with methanol and hexane to remove polar impurities and low molecular weight polymers, **P1** and **P2** were dissolved in $CHCl_3$. The polymers have weight-average molecular weights of 13 800 and 14 200 g mol^{-1}, respectively, with a polydispersity index of 1.6 for both. Although the polymers have similar molecular weights, **P2** displays a higher solubility in $CHCl_3$, toluene, and THF than **P1**, which requires heating to obtain full dissolution. In CH_2Cl_2, **P2** is fully soluble, whereas **P1** is not.

Solution Properties. The optical properties of **P2** were studied by UV−vis absorption, fluorescence, and CD spectroscopy (Figure 1). In xylene solution,[9] the polymer is highly fluorescent with a quantum yield of 0.43.[10] When DMF, a poor solvent for the polymer, is added, only a slight red-shift of the absorbance is observed at xylene/DMF ratios higher than 60/40, along with a small decrease of the fluorescence quantum yield down to 0.28. No CD signal is observed, indicating that the polymer chains are molecularly dissolved. When additional poor solvent is added, a sharp change of optical properties is

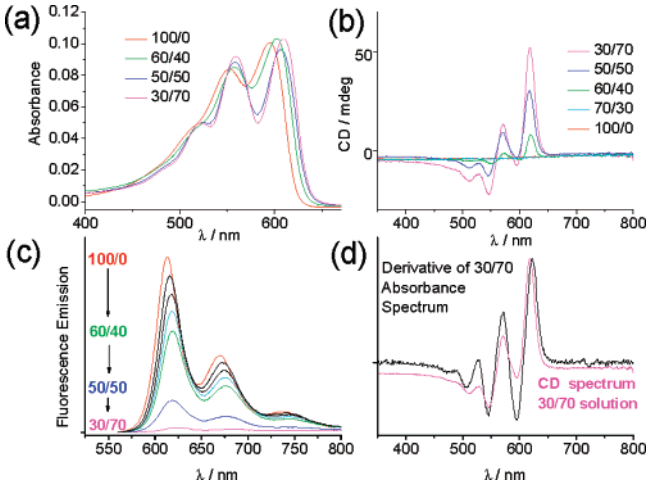

Figure 1. Solvatochromism of **P2** (PProDOT((2*S*)-ethylhexyl)$_2$) in xylene/DMF solutions ($C = 8 \times 10^{-6}$ M): (a) UV absorption; (b) CD spectrum; (c) fluorescence; (d) superposition of the CD spectrum and absorbance derivative of an aggregated 30/70 xylene/DMF solution.

Table 1. Peaks (λ_{max}, nm) and Onsets (in eV) of the Chiral Alkyl PProDOTs Absorption Spectra upon Aggregation Induced by Solvatochromism in Xylene/DMF Solutions

	P1	P2
λ_{max} 100% xylene	556, 603 nm	553, 595 nm
onset 100% xylene	1.98 eV	2 eV
λ_{max} 30% xylene	576, 628 nm	559, 608 nm
onset 30% xylene	1.88 eV	1.95 eV

observed, with a further red-shift of the absorption spectrum by 10 nm. The vibronic features become more resolved, suggesting more ordered, planar chains. In addition, the fluorescence quantum yield drops sharply to less than 0.04 at a 40/60 xylene/DMF ratio. In addition, a strong CD signal corresponding to the $\pi-\pi^*$ absorption appears (Figure 1b). The anisotropy factor in absorption (defined as $\Delta\epsilon/\epsilon$) reaches a maximum of $g_{abs} = 1.8 \times 10^{-2}$ at 625 nm and -1.4×10^{-2} at 498 nm. The signal shape and anisotropy factor in absorption are similar to the CD signals observed in aggregated chiral poly(alkylthiophenes), indicating that PProDOT((2*S*)-ethylhexyl)$_2$ forms similar interchain chiral helices.[11] This is further supported by the planar geometry of the polymer chains, shown by the presence of well-resolved vibronic features in the absorption spectra both in solution and film state. Such planarity of dioxythiophene-based polymers and oligomers is arising from intramolecular sulfur−oxygen interactions along with mesomeric effects.[12] Although the Davydov splitting is not resolved, the close match between the bisignate CD spectrum with the first derivative of the absorption spectrum (Figure 1d) is in full agreement with a splitting of the excited state into two exciton levels via small Davydov interactions, consistent with studies on other polythiophenes.[11]

Solvatochromism on **P1** solutions indicates that **P1** also forms similar chiral interchain aggregates ($g_{abs} = 1.6 \times 10^{-2}$ at 642 nm) with a strong match between the CD spectrum and the first derivative of the absorbance (Supporting Information). However, as shown in Table 1, **P1** displays a stronger bathochromic shift (100 meV) than **P2** (50 meV) upon aggregation.

Complementary thermochromism experiments on 50/50 xylene/DMF solutions of **P1** and **P2** were performed and are presented in Figure 2. At this solvent mixture ratio, both **P1** and **P2** are aggregated at room temperature. Upon heating aggregated solutions of **P2** above 70 °C, the formation of the chiral aggregates is fully reversed to the molecularly dissolved state (Figure 2b). In higher DMF content solutions, the transition to the molecularly dissolved is moved to higher temperatures, becoming irreversible above 60% DMF content. In the case of **P1** in 50/50 xylene/DMF, the aggregates could not be completely reversed to the molecularly dissolved state even at 100 °C (Figure 2a). Aggregated solutions with higher xylene content were also prepared but did not yield full reversibility.

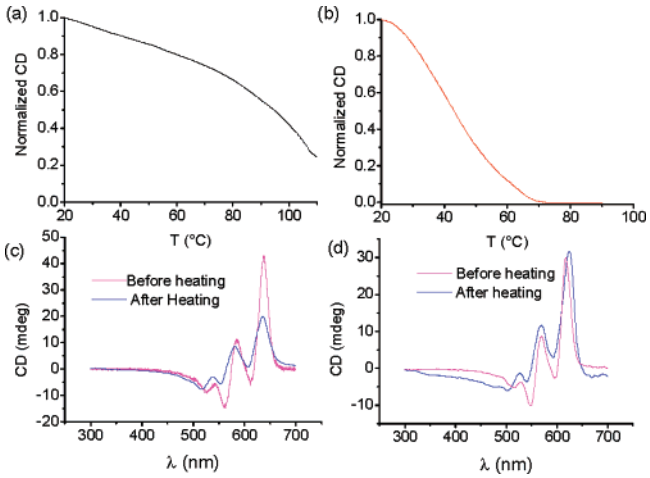

Figure 2. (Top) Temperature-dependent CD intensity of (a) **P1** ($\lambda = 637$ nm) and (b) **P2** ($\lambda = 617$ nm) in 50/50 xylene/DMF mixture ($C = 8 \times 10^{-6}$ M). (Bottom) CD spectrum for (c) **P1** and (d) **P2** in 50/50 xylene/DMF mixture ($C = 8 \times 10^{-6}$ M) as prepared and slowly cooled from 100 °C.

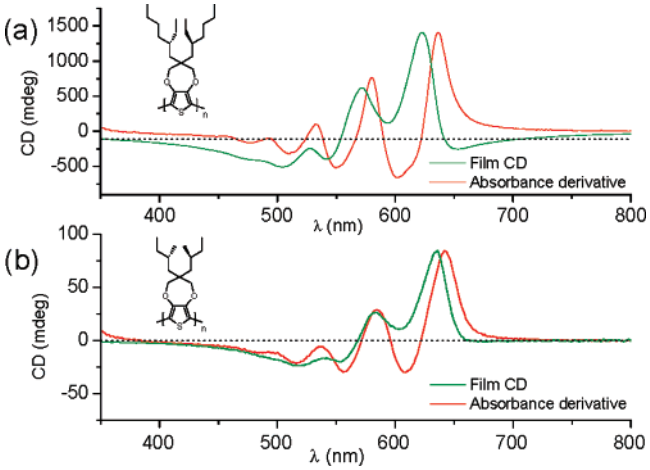

Figure 3. Comparison between CD spectrum and first derivative of the absorption spectrum for **P2** (a) and **P1** (b).

Following the heating cycle to 100 °C, both 50/50 xylene/DMF solutions of **P1** and **P2** were slowly cooled down. In the case of **P2**, molecularly dissolved 100 °C, the aggregates reformed with a full recovery of the CD signal at room temperature (Figure 2d). Solutions of **P1**, remaining aggregated at 100 °C, lead to a significantly decreased CD signal when slowly cooled back to room temperature, indicating an irreversibility and a more complex aggregation process (Figure 2c).[13]

Solid-State Properties. To examine the chiral properties of the polymers in the solid state, films of **P1** and **P2** were spray-coated from toluene. Films of **P2** yield strong CD signals, as presented in Figure 3a. The shape of the CD signals (with maximum anisotropy factors of $g_{abs} = +2.9 \times 10^{-2}$ at 627 nm and -2.2×10^{-2} at 501 nm) is very similar with that in solution, though the absorptions are broadened and red-shifted. Here, the maxima of the CD coincide with those in the UV−vis (Figure 4), which is in contrast to other known polythiophenes.[11,14] As

(9) Xylene used in this study is a mixture of ortho, meta, and para isomers.
(10) Sulforhodamine in absolute ethanol ($\phi = 0.9$) was used as standard.
(11) (a) Langeveld-Voss, B. M. W.; Janssen, R. A. J.; Meijer, E. W. *J. Mol. Struct.* **2000**, *521*, 285−301. (b) Langeveld-Voss, B. M. W.; Janssen, R. A. J.; Christiaans, M. P. T.; Meskers, S. C. J.; Dekkers, H. P. J. M.; Meijer, E. W. *J. Am. Chem. Soc.* **1996**, *118*, 4908−4909.
(12) (a) Grenier, C. R. G.; Pisula, W.; Joncheray, T. J.; Mullen, K.; Reynolds, J. R. *Angew. Chem., Int. Ed.* **2007**, *46*, 714−717. (b) Turbiez, M.; Frere, P.; Allain, M.; Videlot, C.; Ackermann, J.; Roncali, J. *Chem.—Eur. J.* **2005**, *11*, 3742−3752. (c) Apperloo, J. J.; Groenendaal, L.; Verheyen, H.; Jayakannan, M.; Janssen, R. A. J.; Dkhissi, A.; Beljonne, D.; Lazzaroni, R.; Bredas, J. L. *Chem.—Eur. J.* **2002**, *8*, 2384−2396. (d) Spencer, H. J.; Skabara, P. J.; Giles, M.; McCulloch, L.; Coles, S. J.; Hursthouse, M. B. *J. Mater. Chem.* **2005**, *15*, 4783−4792.
(13) (a) Satrijo, A.; Meskers, S. C. J.; Swager, T. M. *J. Am. Chem. Soc.* **2006**, *128*, 9030−9031. (b) Leclere, P.; Surin, M.; Viville, P.; Lazzaroni, R.; Kilbinger, A. F. M.; Henze, O.; Feast, W. J.; Cavallini, M.; Biscarini, F.; Schenning, A. P. H. J.; Meijer, E. W. *Chem. Mater.* **2004**, *16*, 4452−4466.
(14) Langeveld-Voss, B. M. W.; Christiaans, M. P. T.; Janssen, R. A. J.; Meijer, E. W. *Macromolecules* **1998**, *31*, 6702−6704.

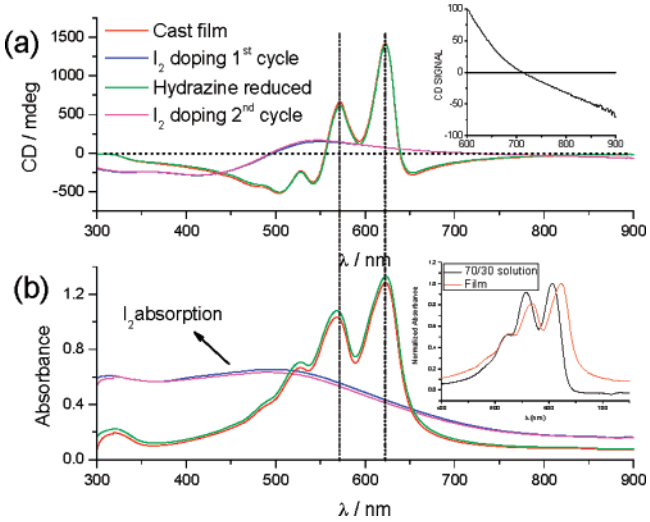

Figure 4. (a) CD and (b) UV−vis absorption spectra evolution with doping (I_2) and undoping (NH_2NH_2 vapor) cycles of **P2** (PProDOT-((2*S*)-ethylhexyl)$_2$) spray-coated films on glass substrates; inset to (a) shows magnification of the 600−900 nm region, and inset to (b) shows the difference in UV absorption between film and aggregated solution.

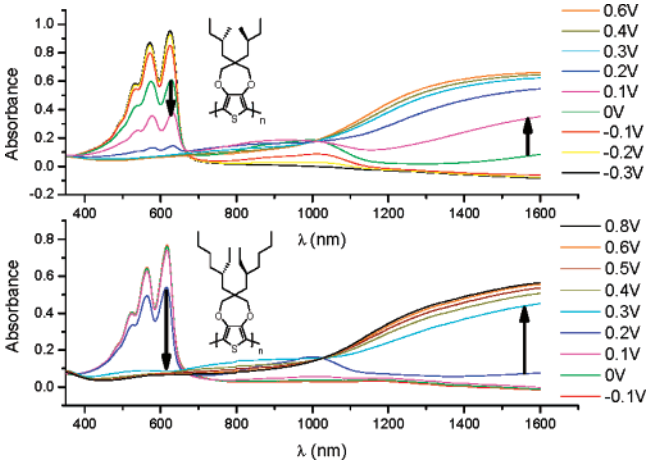

Figure 5. Spectroelectrochemistry of **P1** and **P2** films spray-coated from toluene in 0.1 M TBAP/PC. Potentials are reported against Fc/Fc^+ pseudoreference.

absorption spectroscopy probes all interchain interactions and CD spectroscopy only probes chiral interchain interactions, we speculate that this behavior arises from additional nonchiral interchain interactions between chiral stacks forming during solvent drying. This shift could also originate from the presence of light-scattering effects, frequently observed in chiral polyfluorenes films.[6] The presence of a negative CD signal in films of **P2** at longer wavelength, shown in Figure 3a, would be consistent with this assumption. Spin-coated films of **P2** from *o*-dichlorobenzene (ODCB) also display a CD signal with maxima matching the maxima in the UV−vis spectrum, suggesting that this effect is not strongly affected by the deposition method or the solvent. Spray-coated films of **P1** from toluene also yield a CD signal, but as shown in Figure 3b, it is less intense than **P2**, with maximum anisotropy factor $g_{abs} = +3.2 \times 10^{-3}$ at 637 nm and -1.2×10^{-3} at 512 nm. The decreased anisotropy of **P1** is consistent with the thermochromism result of aggregated solutions showing a more delicate aggregation process for **P1** leading to more heterogeneous aggregates.

Upon exposure of a spray-coated film of **P2** to iodine, the UV−vis spectrum indicates the polymer film is fully oxidized to the bipolaron state (Figure 4b, full spectrum to 1800 nm in the Supporting Information). The corresponding CD signal (Figure 4a), seen in the visible range, is much less intense and blue-shifted compared to that of the neutral film. This suggests that undoped chromophores with short conjugation lengths remain in the film and that the polymer chains retain a chiral orientation in the doped state.[15] A negative CD signal is also observed between 700 and 900 nm (inset of Figure 4a), suggesting the bipolaron band is also CD active. Upon exposure of the films to hydrazine vapor, the neutral polymer CD signal is fully recovered, demonstrating reversibility of the chiral aggregates after an oxidation/charge neutralization cycle. Two days after iodine oxidation, the UV−vis and CD spectra were examined, indicating the polymer was dedoped to the polaron state, as noted by the presence of an absorption peak centered at 950 nm (full spectrum in the Supporting Information). No CD signal is observed for this band showing the polaron absorption is not CD active. Spray-coated films of **P1** also show CD reversibility following iodine doping and hydrazine neutralization cycles (Supporting Information) despite the much lower CD values and limited thermoreversibility of the chiral aggregates in solution.

The above experiment demonstrates that during the casting process, both **P1** and **P2** chains spontaneously self-assemble. The assemblies are reversible upon redox cycling, as no changes in CD signal or shift in absorption spectrum are observed. This result is unique to the branched alkyl PProDOTs as linear alkyl and ether linked alkyl PProDOTs synthesized in our group were shown to retain a "solution conformation" with little or no shift in absorption spectrum during casting.[2,3] For these polymers, a bathochromic shift is only observed upon redox switching and the color of the films changes from a red color to a blue-purple (PProDOT−Hx_2, PProDOT−Bu_2)[2] or a red-purple color (PProDOT(CH_2O-2-ethylhexyl)$_2$).[3]

Spectroelectrochemistry experiments were carried out on **P2** and **P1** (Figure 5). A distinct optical change is observed with a 200 mV potential increase for **P2** as noted by the marked spectra. In the case of **P1**, a wider 350 mV potential window is required to obtain similar optical changes. In PProDOT−Hx_2, the potential window required is even larger, the polymer requiring more than 600 mV to achieve similar optical changes.[3] The band gaps for spray-coated films of **P1** and **P2** are 1.88 and 1.92 eV, respectively, close to the onsets found in aggregated solutions. Cyclic voltammetry at a slow scan rate (5 mV/s) of the two films also indicates an oxidation process over a much larger range of potential in the case of **P1** (Supporting Information). Four point probe conductivity measurements carried out on spray-coated thick films that were gas-phase doped with iodine yielded a conductivity of 4 S cm^{-1} for **P1** and 0.3 cm^{-1} for **P2**.

The sharp optical changes occurring over a narrow range of potential are reminiscent of what was observed in racemic PProDOT(2-ethylhexyl)$_2$. To examine in more detail if the presence of the enantiomerically pure side chains affect the macroscopic properties, the electronic and optical properties of

(15) Koeckelberghs, G.; De Cremer, L.; Vanormelingen, W.; Verbiest, T.; Persoons, A.; Samyn, C. *Macromolecules* **2005**, *38*, 4545−4547.

Table 2. Electronic and Optical Properties of **P2** and Racemic Equivalent

P2	racemic	chiral
$E_{p,a}$ (mV)[a]	45	89
$E_{p,c}$ (mV)[a]	11	43
λ_{max} cast film	618, 564, 523	617, 564, 524
E_g (optical, eV)	1.93	1.92
conductivity (S cm^{-1})[b]	0.4	0.3

[a] CV-determined anodic and cathodic peak potentials of drop-cast films on a Pt button electrode measured in 0.1 M tetrabutylammonium perchlorate/acetonitrile electrolyte vs Fc/Fc$^+$. [b] Gas-phase doped with iodine for 1 h.

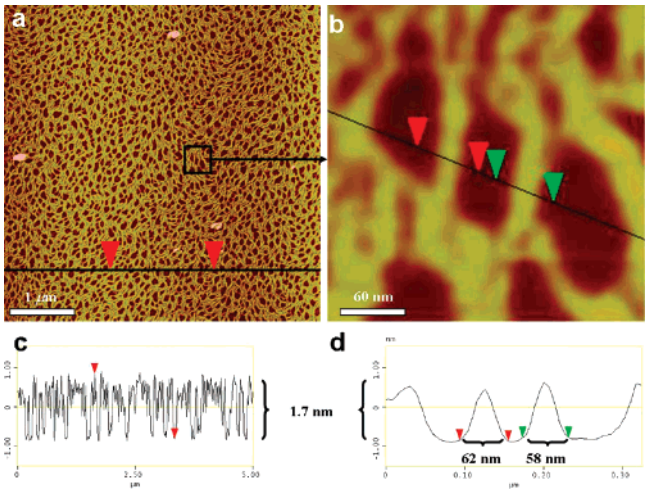

Figure 6. AFM topographic image of a film of **P1** spin-coated at 2000 rpm from a 0.2 mg/mL ODCB solution. Bright regions correspond to the polymer and dark regions to the mica surface: (a) 5 × 5 μm^2; (b) magnification, 300 × 300 nm^2; (c) height profile of the cross section shown in (a); (d) cross section of (b) showing the width of selected fibers.

both polymers were compared. As presented in Table 2 for **P2**, the properties of both racemic and chiral polymers are found to be almost identical, showing that the enantiomeric purity has little or no effect on the macroscopic properties.

Morphology Studies. In the previous sections, we have examined the microscopic ordering of the two chiral polymers. CD experiments show that the (2*S*)-ethylhexyl polymer **P2**, although having more bulky side chains, displays strong microscopic ordering both in aggregated solution and the solid state. Surprisingly, the polymer was found to have an order of magnitude lower conductivity than **P1**.

To explain this difference, we examined the two polymers morphologies by AFM. Films of **P1** and **P2** were both spin-coated onto a mica surface from a 0.2 mg/mL solution in 1,2-dichlorobenzene (2000 rpm). AFM study of **P1** films reveals the presence of interconnected nanoribbons (Figure 6). The individual ribbons have an average height of 1.7 nm and average width of 50 nm (dimensions after correction for tip-broadening effect[16]). The height of the ribbons is compatible with the height of the **P1** chains, estimated between 1.4 and 2 nm for chains with trans conformation of adjacent thiophenes and an extended conformation for the alkyl chains.[17] The width of the ribbons largely exceeds the length of the chains expected from the GPC data yielding an estimated length of 11−15 nm for **P1** chains.

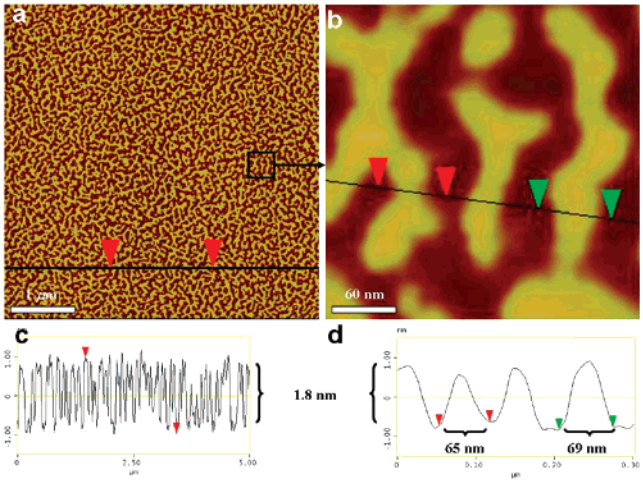

Figure 7. AFM topographic image of a film of **P2** spin-coated at 2000 rpm from a 0.2 mg/mL ODCB solution. Bright regions correspond to the polymer fibers and dark regions to the mica surface: (a) 5 × 5 μm^2; (b) magnification, 300 × 300 nm^2; (c) height profile of the cross section shown in Figure 6a; (d) cross section of Figure 6b showing the width of selected fibers.

This observation suggests that the nanoribbons are formed of stacks of interpenetrated chains, perpendicular to the mica surface. The interconnected network of ribbons extends over several micrometers (Figure 6a and 6b).

In the case of **P2**, nanoribbons are also observed (Figure 7), with an average height for individual ribbons of 1.8 nm, fully compatible with the calculated height of 1.5−2.2 nm. The ribbons have widths, after tip correction,[16] of 50−60 nm. The ribbons, however, extend to a much shorter range, typically 250−500 nm, and are poorly connected together as shown in Figure 7, parts a and b. Such a difference in morphology could explain the difference in conductivity between the two polymers. In poly(3-hexylthiophene) (P3HT), increasing evidence suggests that the increase of charge mobility with increasing molecular weight arises from a high degree of interconnectivity between small, highly ordered domains.[18]

Conclusions

In conclusion, we introduce a powerful and versatile synthesis to prepare the most often used enantiomerically pure side chains which solubilize π-conjugated polymers. Using this method, we synthesized a functionalized poly(3,4-propylenedioxythiophene) **P2** having two chiral ethylhexyl side chains and compared its properties to the chiral methylbutyl derivative **P1**. The enantiomerically pure side chains allow us to follow the aggregation process by CD spectroscopy, as the two polymer forms chiral helical aggregates similar to chiral alkyl polythiophenes. CD analysis of the more soluble **P2** indicates that the bulkier side chains allow for a greater control of the microscopic ordering in aggregated solution. CD experiments on films of **P1** and **P2** also suggest that **P1** forms more heterogeneous aggregates than **P2**. For both polymers, the chiral aggregates were found to be fully reversible upon chemical oxidation and reneutralization cycles.

(16) Samori, P.; Francke, V.; Mangel, T.; Mullen, K.; Rabe, J. P. *Opt. Mater.* **1998**, *9*, 390−393.
(17) Width of the chains, estimated using Hyperchem software is given as a range as it is dependent on the conformation of the seven-membered ring.
(18) (a) Kline, R. J.; McGehee, M. D.; Kadnikova, E. N.; Liu, J. S.; Frechet, J. M. J.; Toney, M. F. *Macromolecules* **2005**, *38*, 3312−3319. (b) Brinkmann, M.; Rannou, P. *Adv. Funct. Mater.* **2007**, *17*, 101−108. (c) Yang, H. C.; Shin, T. J.; Yang, L.; Cho, K.; Ryu, C. Y.; Bao, Z. N. *Adv. Funct. Mater.* **2005**, *15*, 671−676.

The differences in microscopic ordering could explain the broader potential window required for obtaining complete optical changes during oxidation. However, such differences are unlikely to account for the lower conductivities of **P2** films. The lower conductivities are rather explained by different morphologies of the polymer films, as **P1** forms an interconnected network of nanoribbons, whereas **P2** forms more isolated nanoribbons.

Acknowledgment. We gratefully acknowledge funding of this project from the AFOSR (Grant FA9550-06-1-0192).

Supporting Information Available: Full synthetic procedures and characterization, along with absorbance, emission, and CD spectra for PProDOT((2*S*)-methylbutyl)$_2$). This material is available free of charge via the Internet at http://pubs.acs.org.

JA068461T